

See discussions, stats, and author profiles for this publication at: <https://www.researchgate.net/publication/244402546>

# The Complexation of Tetracycline and Anhydrotetracycline with $Mg^{2+}$ and $Ca^{2+}$ : A Spectroscopic Study

ARTICLE *in* THE JOURNAL OF PHYSICAL CHEMISTRY B · NOVEMBER 1998

Impact Factor: 3.3 · DOI: 10.1021/jp9824050

---

CITATIONS

97

---

READS

118

4 AUTHORS, INCLUDING:



Wilfried Szymczak

Helmholtz Zentrum München

30 PUBLICATIONS 739 CITATIONS

SEE PROFILE

# The Complexation of Tetracycline and Anhydrotetracycline with $\text{Mg}^{2+}$ and $\text{Ca}^{2+}$ : A Spectroscopic Study

J. M. Wessels,<sup>\*,†</sup> W. E. Ford,<sup>‡</sup> W. Szymczak,<sup>§</sup> and S. Schneider<sup>||</sup>

GSF-Flow Cytometry Group, 85764 Neuherberg, Germany, Folly Beach, South Carolina, GSF-Institute of Radiation Protection, 85764 Neuherberg, Germany, Institut für Physikalische und Theoretische Chemie, Universität Erlangen-Nürnberg, 91058 Erlangen, Germany

Received: May 28, 1998

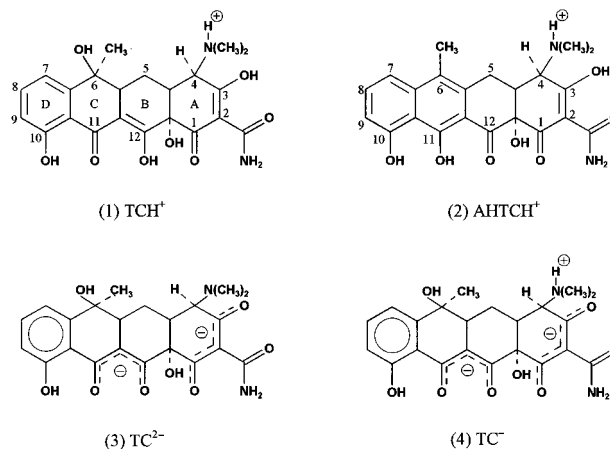
Steady-state absorption and emission, circular dichroism (CD), and time-of-flight secondary-ion-mass-spectroscopic (TOF–SIMS) measurements were performed to study the complexation of tetracycline (TC) and anhydrotetracycline (AHTC) with  $\text{Mg}^{2+}$  and  $\text{Ca}^{2+}$  ions, respectively, in aqueous solutions at pH 8.02. The results obtained suggest that  $\text{Ca}^{2+}$  forms a 1:2 ligand:metal complex with TC via chelation through O10–O11 and O12–O1 and induces thereby the extended conformation A of TC, which is stabilized through hydrogen bonding between the deprotonated dimethylamino nitrogen, N4, and OH12a. pH titrations provide evidence that N4 deprotonates in the presence of a 164-fold molar excess of  $\text{Ca}^{2+}$  at approximately pH  $\geq 7.7$  ( $c_{\text{TC}} = 2.1 \times 10^{-5} \text{ M}$ ). In contrast to  $\text{Ca}^{2+}$ ,  $\text{Mg}^{2+}$  binds to N4–O3 and thereby stabilizes the twisted conformation B of TC. TOF–SIMS measurements indicate that a 1:2 ligand:metal complex is formed in addition to the 1:1 complex. The  $\text{Mg}^{2+}$ -induced increase in the fluorescence intensity and the observed changes in the absorption spectra provide evidence that the other  $\text{Mg}^{2+}$  ion binds to the BCD ring system through the deprotonated O11. In contrast to TC, which adopts the twisted conformation B in aqueous solution at pH 8.02, AHTC exhibits the extended conformation A due to slightly lower deprotonation constants. In the presence of  $\text{Mg}^{2+}$ , however, the conformational equilibrium is shifted toward the twisted conformation B due to binding of  $\text{Mg}^{2+}$  to N4. TOF–SIMS measurements suggest that a 2:2 ligand:metal complex is formed. AHTC remains in conformation A upon addition of  $\text{Ca}^{2+}$ ; complexation through O10 can be excluded on the basis of absorption spectroscopic data.

## 1. Introduction

Tetracyclines (TCs) (Scheme 1) form reversible complexes with metal ions as well as with substances of low and high molecular weight. The complexation behavior determines to a large extent their biological action.<sup>1–3</sup> The complex deprotonation pattern of TCs as well as the large number of possible chelation sites has led to extensive studies on the complexation of various TC derivatives with several different metal ions in aqueous and organic environments using nuclear magnetic resonance spectroscopy,<sup>1,4–7</sup> circular dichroism spectroscopy,<sup>1,8–17</sup> absorption and fluorescence spectroscopy,<sup>1,2,18,19</sup> as well as electroanalytical methods.<sup>20–22</sup>

It has been established that TCs can exist in different conformations, depending on the substituents, metal chelation, and the solvent used. In neutral to acidic solutions TC adopts a twisted conformation, where the dimethylamino group lies above the BCD ring system in order to relieve the steric crowding between the protonated nitrogen of the dimethylamino group,  $\text{NH}_4^+$ , and OH12a, which is also referred to as conformation B (Scheme 2).<sup>6,11</sup> In basic or nonaqueous solutions the

## SCHEME 1: Chemical Structures and Abbreviations Used



equilibrium is shifted to the extended conformation—also designated conformation A—where the dimethylamino group lies below the plane spanned by the BCD ring system (Scheme 2).<sup>9</sup> This conformation is stabilized by strong hydrogen bonding between the deprotonated N4 and OH12a.<sup>23,24</sup> The driving force for the interchange between the two conformations as  $\text{H}_2\text{O}$  is replaced by nonaqueous solutions is the increase in the ammonium group acidity and O3 basicity. It has been proposed that the equilibrium between these two conformers in polar and nonpolar media plays an important role in the pharmacokinetic properties of TCs.<sup>14,26,27</sup>

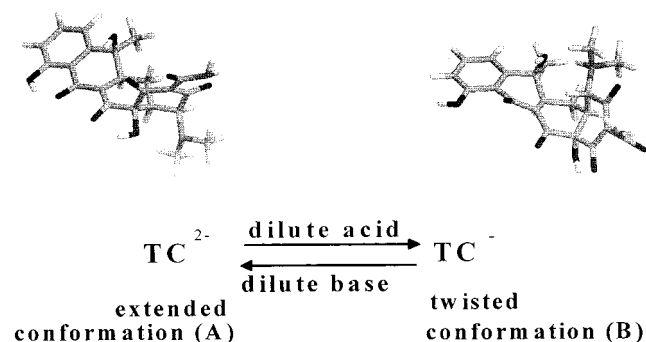
\* Author to whom correspondence should be addressed at Siegfried Schneider Institut für Physikalische und Theoretische Chemie, Universität Erlangen-Nürnberg, Egerlandstrasse 3, D-91058 Erlangen, Germany. Phone: 0049-9131-857340. Fax: 0049-9131-858307. E-mail: schneider@pctc.chemie.uni-erlangen.de.

<sup>†</sup> GSF-Flow Cytometry Group.

<sup>‡</sup> Folly Beach, SC.

<sup>§</sup> GSF-Institute of Radiation Protection.

<sup>||</sup> Institute für Physikalische und Theoretische Chemie.

**SCHEME 2: Protonation of TC<sup>2-</sup> with Concomitant Change of Conformation**

TCs exhibit three macroscopic acidity constants, the assignments of which have been widely accepted. In aqueous environments the first deprotonation ( $pK_1 \sim 3\text{--}4$ ) occurs at OH3. The second  $pK$  value is attributed to OH12 ( $pK_2 \sim 7.3\text{--}8.1$ ), and the third one to the protonated nitrogen of the dimethylamino group ( $pK_3 \sim 8.8\text{--}9.8$ ).<sup>25,28</sup> Since chelation occurs predominantly at basic sites and metal ions prefer O and N donors, the possible binding sites depend on the nature of the solvent and the pH value.<sup>25</sup>

Although a variety of techniques have been used to study the complexation behavior of TC and various derivatives, the results obtained have led to partly contrary assignments of the chelation sites. Depending on the chosen experimental conditions, i.e., nature of the solvent, pH as well as ligand:metal ratio, TCs can form complexes exhibiting a 2:1, 1:1, or a 1:2 ligand:metal stoichiometry. For example, Newman and Frank studied the complexation of TC and structurally modified TC where potential complexation sites were blocked.<sup>12</sup> Comparisons of CD spectra obtained from dedimethylaminotetracycline and 2-cyanotetracycline in the presence of  $\text{Ca}^{2+}$  and  $\text{Mg}^{2+}$  ions in 1:1 MeOH:H<sub>2</sub>O suggested that neither the N4 nor the amide group at C2 is involved in the complexation with TC. The evaluation of stability constants for the coordination of TC in comparison with tetracycline betaine having three methyl groups at N4 also supported the conclusion of Newman and Frank.<sup>29</sup> In contradiction to these results, Mitscher et al. suggested that below pH 7.5  $\text{Ca}^{2+}$  and  $\text{Mg}^{2+}$  bind to the BCD ring system, while above pH 7.5 a second  $\text{Ca}^{2+}$  binds through N4 and OH12a.<sup>11</sup> According to Lambs et al. the plasma-relevant complexes are 1:1 and 1:2 ligand:metal complexes and the proposed chelation sites for  $\text{Ca}_2\text{TC}$  are N4–OH12a and O10–O12, while for  $\text{Mg}_2\text{TC}$  they are N4–O3 and O10–O12.<sup>15</sup> Williamson and Everett suggested that complexation occurs at the tricarbonyl methane moiety when DMSO is used as a solvent.<sup>4</sup> Similar discrepancies regarding the assignments of the chelation sites for  $\text{Cu}^{2+}$  and  $\text{Co}^{2+}$  can be found in the literature.<sup>16,18,20</sup>

Anhydrotetracycline (AHTC) is one of the toxic degradation products of tetracycline. The complexation of AHTC with divalent cations has also been the subject of investigations since it is often used as an affector.<sup>17,30,31</sup> AHTC exhibits a reduced antibiotic activity but shows an approximately 35-fold stronger binding to the TetR protein compared to TC, indicating that the ribosome recognition of both drugs differs.<sup>32</sup>

With respect to the microbiological action of TCs,  $\text{Mg}^{2+}$  and  $\text{Ca}^{2+}$  are probably the most relevant divalent cations to be considered for chelation. The concentrations of  $\text{Mg}^{2+}$  and  $\text{Ca}^{2+}$  ions in the blood plasma (pH 7.4) are approximately 1.3 and 0.9 mM, respectively.  $\text{Mg}^{2+}$  is the dominant divalent cation

( $c = 2$  mM) in the intracellular environment ( $\text{pH} \leq 6.6$ ), where the concentration of  $\text{Ca}^{2+}$  is significantly lower ( $c = 0.1 \mu\text{M}$ ).<sup>32</sup>

In view of the above-described uncertainties regarding the complexation of TCs with divalent metal ions and the importance of their complexation behavior regarding their biological action we entered into a more extensive investigation of the complexation of TC (1) and AHTC (2) (Scheme 1) with  $\text{Ca}^{2+}$  and  $\text{Mg}^{2+}$  ions focusing on physiologically relevant conditions, i.e., aqueous solution between pH 7 and 8, using steady-state absorption and emission spectroscopy as well as CD spectroscopy. In addition, time-of-flight secondary-ion-mass-spectroscopic measurements were performed in order to gain further information about the complexation behavior of TC and AHTC.

## 2. Experimental Section

**2.1. Chemicals.** Tetracycline hydrochloride (TC) obtained from Fluka (Germany) and anhydrotetracycline hydrochloride (AHTC) from Acros Chimica (Germany) were used without further purification. TC ( $c < 5 \times 10^{-5}$  M) and AHTC ( $c < 2.2 \times 10^{-5}$  M) were dissolved in a 50 mM TRIS buffer (pH 8.02) containing 0.15 M NaCl. Stacking interactions, which have been observed for TCs particularly in the D-ring region, can be neglected at these concentrations.<sup>8</sup>  $\text{MgSO}_4$  and  $\text{CaCl}_2$  were added from a stock solution at the desired concentration. All experiments were carried out at room temperature ( $20 \pm 1$  °C) using freshly prepared solutions which were kept in the dark.

**2.2. Steady-State Spectroscopic Studies.** UV-VIS absorption spectra were measured with a wavelength resolution of  $\Delta\lambda = \pm 2$  nm using a Hewlett-Packard diode array spectrometer. Steady-state fluorescence emission measurements were performed using the LS55B (Perkin-Elmer) fluorescence emission spectrometer. The excitation and emission slit widths were set to a bandwidth of 10 and 5 nm, respectively. The fluorescence of all samples was excited either at the isosbestic point or at a wavelength where the variations in the OD of the absorption spectra were minimal. In the latter case the fluorescence intensities were corrected for the absorbance differences at the excitation wavelength. The circular dichroism spectra were measured using a Jobin Yvon CD6 spectrometer with a resolution of  $\Delta\lambda = \pm 1$  nm. The optical density of the samples varied between  $0.4 \leq \text{OD} \leq 0.7$  at  $\lambda_{\text{max}}$ .

**2.3. TOF-SIMS Measurements.** Time-of-flight secondary-ion-mass-spectroscopic (TOF-SIMS) measurements<sup>33</sup> were performed using a pulsed 25 keV  $\text{SF}_5^+$  beam. The emitted secondary ions were extracted and accelerated with +3 kV (positive SIMS mode). After a drift length of 60 cm the secondary ions were stopped and detected with a three-stage multichannel plate detector (Hamamatsu F4655). The detector signals were analyzed using a fast time-to-digital converter (FAST 7886). Up to  $3 \times 10^6$  spectra in the mass regime  $0 \leq m/u \leq 3000$  were added up. Based on the calibration, the mass is determined with an uncertainty of  $m/u \leq 0.5$  in the mass region  $\leq 1000$  u.

The samples were prepared on cleaned silicon disks (5 mm  $\times$  5 mm) cut from polished wafers of standard industrial quality onto which a submonolayer of C was sputtered. A 10  $\mu\text{L}$  droplet was deposited on the surface and either dried under air or excess solvent was removed after an adsorption period of 5 min using a microtip.

## 3. Results

**3.1. Tetracycline Titration with  $\text{Ca}^{2+}$  at pH 8.02.** Figure 1, parts a and b, show CD spectra of TC ( $2.1 \times 10^{-5}$  M)

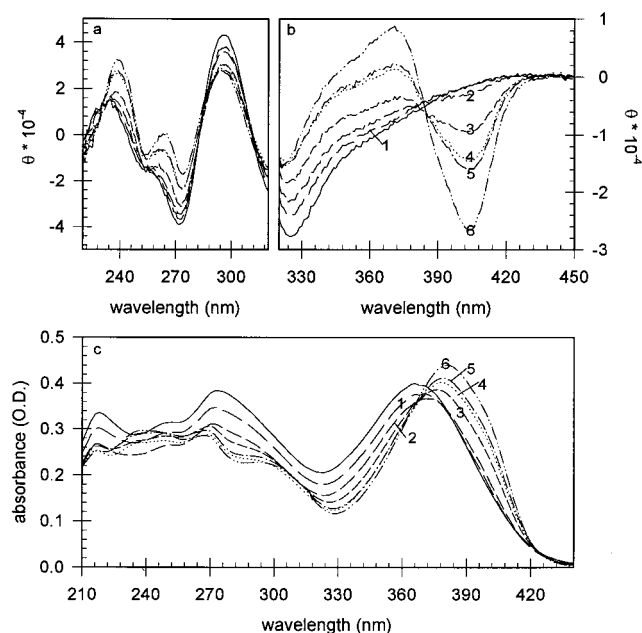


**Figure 1.** CD spectra (a, b) and absorption spectra (c) of TC ( $2.1 \times 10^{-5}$  M) in the absence (solid line) and in the presence of increasing  $\text{Ca}^{2+}$  concentrations. The molar ratios of TC: $\text{Ca}^{2+}$  are (1) 1:7.9, (2) 1:15.8, (3) 1:47, (4) 1:79, (5) 1:158, and (6) 1:626.

recorded in the presence of increasing  $\text{Ca}^{2+}$  concentrations. The molar ratio TC: $\text{Ca}^{2+}$  varies between 1:0 and 1:626. Increasing the  $\text{Ca}^{2+}$  concentration results in the formation of two new Cotton effects, one in the UV (Figure 1a) and one in the visible (Figure 1b). This is expected if chelation with  $\text{Ca}^{2+}$  causes a conformational change of TC (see also discussion below). The CD spectra obtained from samples with molar ratios TC: $\text{Ca}^{2+} \geq 1:79$  exhibit an isosbestic point at about 384 nm (traces 4–6), while the spectra obtained from samples with TC: $\text{Ca}^{2+} < 1:79$  show no clear isosbestic point. The  $\text{Ca}^{2+}$ -induced changes in the CD signal intensity evaluated at 263 and 404 nm are summarized in Figure 2a.

The absorption spectra of the same samples are depicted in Figure 1c. A bathochromic shift of the long-wavelength absorption band from 366 nm in the absence of  $\text{Ca}^{2+}$  to 382 nm at a 626-fold molar excess of  $\text{Ca}^{2+}$  is observed. Up to molar ratios of TC: $\text{Ca}^{2+} = 1:15.8$  the shift is accompanied by a decrease in the extinction coefficient, while at molar ratios TC: $\text{Ca}^{2+} > 1:15.8$  an increase of the extinction coefficient is observed (Figure 1c). The absorption spectra show two isosbestic points—at about 382 nm for molar ratios TC: $\text{Ca}^{2+} \leq 1:15.8$  and at about 366 nm for TC: $\text{Ca}^{2+} \geq 1:15.8$ . In addition, distinct alterations are observed in the UV range. At molar ratios TC: $\text{Ca}^{2+} \geq 1:47$  a splitting of the absorption maximum at 274 nm into two bands is indicated by the formation of a pronounced shoulder. The formation of a new absorption band centered at about 240 nm is also detected. The optical densities evaluated at 274 and 382 nm show both one inflection point in TC: $\text{Ca}^{2+}$  regimes below and above 1:15.8 (Figure 2b).

The broad fluorescence emission band of TC peaks at about 503 nm and exhibits a slight shoulder at about 523 nm. Upon addition of  $\text{Ca}^{2+}$  the weak fluorescence intensity increases and the shoulder becomes slightly more pronounced (data not shown). Addition of a 164 molar excess of  $\text{Ca}^{2+}$  leads to an approximately 7-fold increase in the integrated fluorescence intensity ( $I_{\text{INT}}$ ) (Figure 2c).

**3.2. pH-Titration of TC in the Presence of  $\text{Ca}^{2+}$  at a Molar Ratio TC: $\text{Ca}^{2+} = 1:164$ .** The CD-spectra obtained from

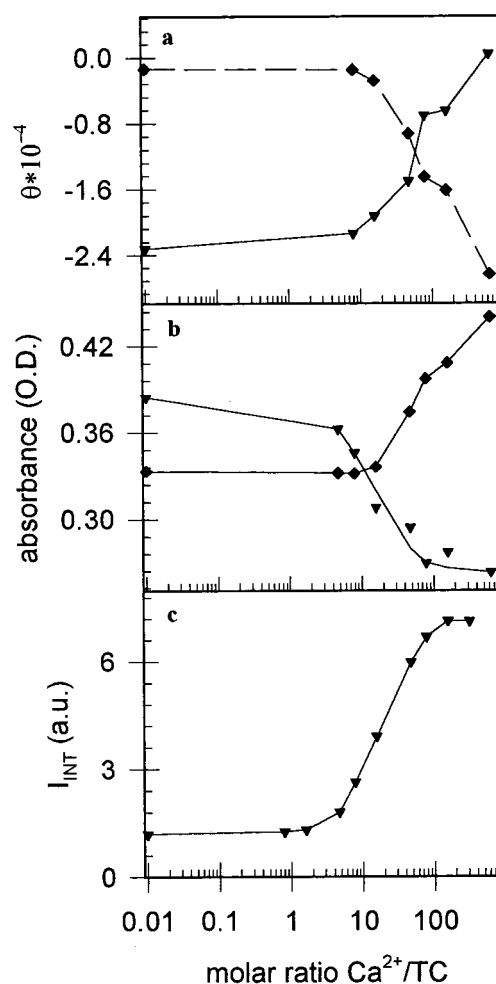


**Figure 2.** (a) CD-signal intensity of TC: $\text{Ca}^{2+}$  solutions as a function of the molar ratio  $\text{Ca}^{2+}/\text{TC}$  ( $c_{\text{TC}} = 2.1 \times 10^{-5}$  M) evaluated at 263 nm ( $\blacktriangledown$ ) and at 404 nm ( $\blacklozenge$ ). (b) Optical density of TC: $\text{Ca}^{2+}$  solutions as a function of the molar ratio  $\text{Ca}^{2+}/\text{TC}$  evaluated at 274 nm ( $\blacktriangledown$ ) and at 382 nm ( $\blacklozenge$ ). (c) Integrated fluorescence intensity ( $I_{\text{INT}}$ ) of TC: $\text{Ca}^{2+}$  solutions ( $\lambda_{\text{exc}} = 305$  nm) as a function of the molar ratio  $\text{Ca}^{2+}/\text{TC}$ .

the titration ( $8.02 \geq \text{pH} \geq 7.12$ ) of TC samples in the presence of a 164-fold molar excess of  $\text{Ca}^{2+}$  ions are shown in Figure 3a,b. A decrease of the pH causes the two  $\text{Ca}^{2+}$ -induced Cotton effects to disappear. The above-described alterations in the absorption spectra (section 3.1) disappear also as the pH decreases (spectra not shown). The long-wavelength absorption band shifts from 382 nm at pH 8.21 (TC: $\text{Ca}^{2+} = 1:164$ ) to 364 nm at pH 5.91 (TC: $\text{Ca}^{2+} = 1:164$ ), and there is a concomitant decrease in the extinction coefficient. As in the case of the  $\text{Ca}^{2+}$  titration at pH 8.02 (Figure 1c), isosbestic points at 352 nm ( $5.9 \leq \text{pH} \leq 7.5$ ) and at 372 nm ( $\text{pH} \geq 7.5$ ) are observed (data not shown). In addition, at pH  $< 7.5$  the above-described spectral alterations in the UV region disappear.

The fluorescence emission spectra of the solutions excited at  $\lambda_{\text{exc}} = 305$  nm and  $\lambda_{\text{exc}} = 365$  nm are depicted in Figure 3, parts c and d, respectively. With  $\lambda_{\text{exc}} = 305$  nm, the integrated fluorescence intensity ( $I_{\text{INT}}$ ) increases 4-fold as the pH is raised from pH 5.9 to pH 7.93, then remains essentially constant up to pH 8.32 (Figure 3e). Below pH 7.34 the emission spectrum has a maximum at 502 nm and a shoulder near 523 nm. This shoulder becomes more pronounced at pH  $\geq 7.34$ , and the spectra obtained at pH  $\geq 7.93$  have their maximum at 523 nm (Figure 3f). Similar changes are observed with  $\lambda_{\text{exc}} = 365$  nm (Figure 3d).



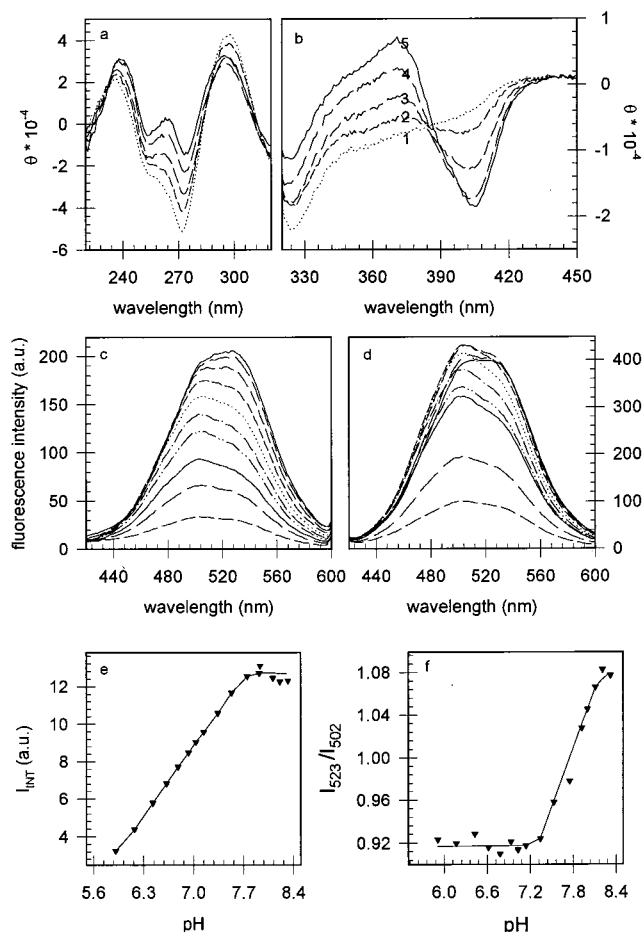


**Figure 3.** CD-spectra (a, b) of TC ( $2.1 \times 10^{-5}$  M) in the presence of a 164 molar excess of  $\text{Ca}^{2+}$  at  $7.29 \leq \text{pH} \leq 8.02$ : (1) pH 7.29, (2) pH 7.51, (3) pH 7.73, (4) 7.93, and (6) 8.02. Fluorescence emission spectra of TC: $\text{Ca}^{2+}$  = 1:164 excited at 305 nm (c) and at 365 nm (d) at pH 5.9, pH 6.43, pH 6.78, pH 7.03, pH 7.14, pH 7.35, pH 7.75, pH 7.93, pH 8.12, and pH 8.32, respectively (from the bottom to the top). (e) Integrated fluorescence intensity ( $I_{\text{INT}}$ ) of TC: $\text{Ca}^{2+}$  = 1:164 solutions ( $\lambda_{\text{exc}}$  = 305 nm) as a function of the pH. (f) Fluorescence intensity ratio ( $I_{532}/I_{502}$ ) of TC: $\text{Ca}^{2+}$  = 1:164 solutions ( $\lambda_{\text{exc}}$  = 305 nm) as a function of the pH.

**3.3. Tetracycline Titration with  $\text{Mg}^{2+}$  at pH 8.02.** Figure 4 a,b shows the CD spectra of TC in the presence of various concentrations of  $\text{Mg}^{2+}$  ( $1:0 \leq \text{TC}:\text{Mg}^{2+} \leq 1:396$ ). In contrast to the spectral changes observed with  $\text{Ca}^{2+}$ , the addition of  $\text{Mg}^{2+}$  does not result in the formation of new Cotton effects. The intensity of the negative absorption band at 272 nm decreases further upon addition of  $\text{Mg}^{2+}$ , indicating that chelation with  $\text{Mg}^{2+}$  stabilizes the conformation of TC present at pH 8.02 (Figure 4a). In addition, the formation of a shoulder in the visible region is observed (Figure 4b).

Titration with  $\text{Mg}^{2+}$  leads also to a shift of the long-wavelength absorption band from 366 nm in the absence of  $\text{Mg}^{2+}$  to 374 nm at a molar ratio TC: $\text{Mg}^{2+}$  = 1:260 (Figure 4c). The bathochromic shift is accompanied by an increase in the extinction coefficient (Figure 4d). In addition, at molar ratios TC: $\text{Mg}^{2+}$  > 1:64 the formation of a slight shoulder at about 392 nm is observed. The absorption spectra exhibit two isosbestic points at about 346 and 410 nm. Furthermore, with increasing  $\text{Mg}^{2+}$  concentration an increase in absorbance between 220 nm  $\leq \lambda \leq$  280 nm is observed (Figure 4c). The integrated fluorescence intensity ( $I_{\text{INT}}$ ) increases upon addition of  $\text{Mg}^{2+}$  by a factor of approximately 12 (Figure 4e), while the

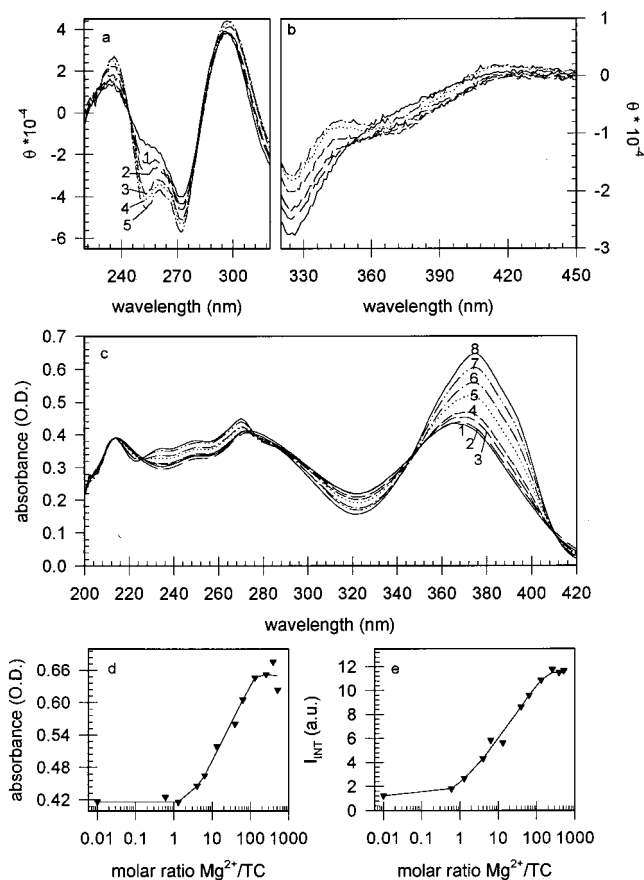


**Figure 4.** CD-spectra (a, b) of TC ( $2.1 \times 10^{-5}$  M) in the absence (solid line) and in the presence of increasing  $\text{Mg}^{2+}$  concentrations. The molar ratios of TC: $\text{Mg}^{2+}$  are (1) 1:6.6, (2) 1:13.3, (3) 1:40, (4) 1:133, and (5) 1:396 (c) Absorption spectra of TC: $\text{Mg}^{2+}$  solutions exhibiting molar ratios of (1) 1:0, (2) 1:1.3, (3) 1:4, (4) 1:6.4, (5) 1:39.6, (6) 1:64, (7) 1:132, and (8) 1:260. (d) Optical density of TC: $\text{Mg}^{2+}$  solutions evaluated at 374 nm as a function of the molar ratio  $\text{Mg}^{2+}/\text{TC}$ . (e) Integrated fluorescence intensity ( $I_{\text{INT}}$ ) of TC: $\text{Mg}^{2+}$  solutions ( $\lambda_{\text{exc}}$  = 346 nm) as a function of the molar ratio  $\text{Mg}^{2+}/\text{TC}$ .

shape of the emission spectrum remains unchanged (data not shown).

**3.4. TOF-SIMS Measurements of TC in the Presence of  $\text{Mg}^{2+}$  and  $\text{Ca}^{2+}$ .** Figure 5 shows the positive TOF-SIMS spectra of TC (Figure 5a), TC with  $\text{Mg}^{2+}$  (Figure 5b), and TC with  $\text{Ca}^{2+}$  (Figure 5c) in the mass region  $440 \leq m/u \leq 600$ . The major peak of the TC sample at  $m/u$  = 445.4 can be attributed to the protonated form of TC ( $\text{TC}^{\text{H}^+}$ ). The observed peak structures are due to the contribution of isotopes. Carbon is the only atom in TC exhibiting a significant portion of a second isotope, and the calculated isotope pattern of  $\text{C}_{22}$  accounts for the observed peak structure (Figure 5b). In addition a peak at  $m/u$  = 467.4 is detected which can be attributed to chelation of TC with  $\text{Na}^+$  leading to a complex of the form  $[\text{TC} + \text{Na}^+]^+$  (Figure 5a). Chelation of  $\text{Na}^+$  with TC has also been observed by Gulbis et al. in NMR studies.<sup>34</sup> In the presence of a 372-fold molar excess of  $\text{Mg}^{2+}$  three peaks are detected at  $m/u$  = 484.5, 507.3, and 528.2. The peaks at  $m/u$  = 484.5 and at  $m/u$  = 507.3 correspond to a 1:1 and 1:2 ligand to metal complex of the forms  $[\text{TC}^{2-} + \text{Mg}^{2+} + \text{H}_2\text{O}^+]^+$  and  $[\text{TC}^{2-} + 2\text{Mg}^{2+} + \text{OH}^-]^+$ , respectively. The calculated isotope patterns of  $\text{C}_{22} + \text{Mg}$  and  $\text{C}_{22} + 2\text{Mg}^{2+}$  represent the negative slopes of both peaks (Figure 5d). The mass difference between the second (507.3 u) and third peak (528.2 u) suggests that this peak is due to a complex where a  $\text{H}^+$  is exchanged with a  $\text{Na}^+$ . In the presence of a 372-fold molar excess of  $\text{Ca}^{2+}$

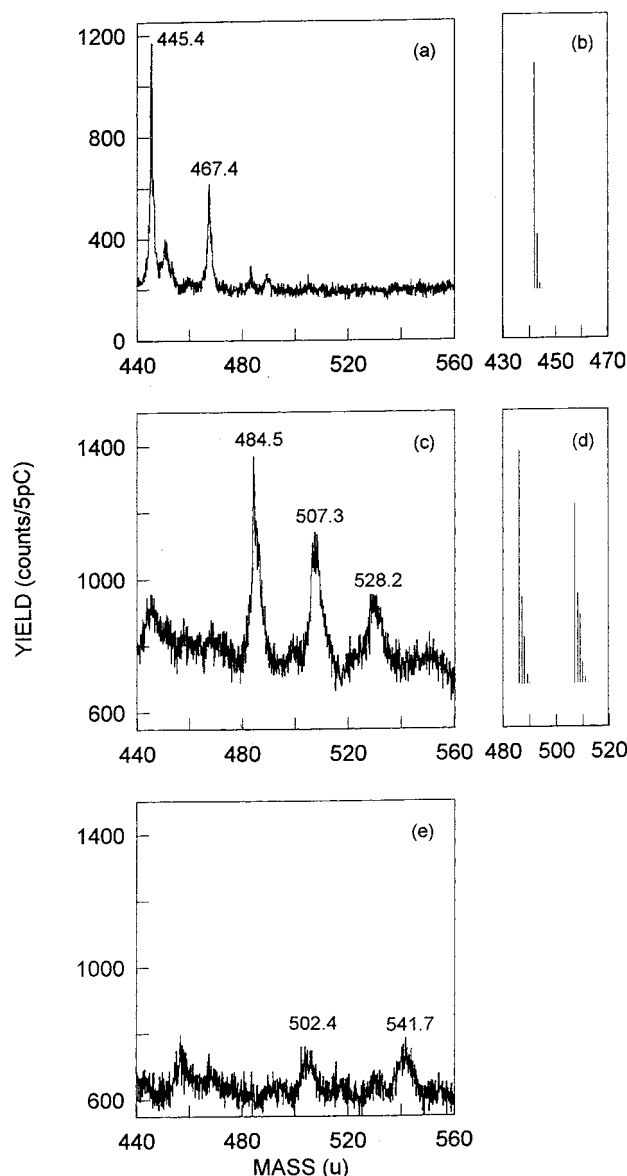


**Figure 5.** Positive TOF-SIMS spectra of TC ( $2.1 \times 10^{-5}$  M) (a), the calculated isotope pattern of  $\text{C}_{22}$  normalized to the observed signal intensity (b),  $\text{TC}:\text{Mg}^{2+} = 1:372$  (c), the calculated isotope patterns of  $\text{C}_{22}\text{Mg}_1$  and  $\text{C}_{22}\text{Mg}_2$  normalized to the observed signal intensities (d), and  $\text{TC}:\text{Ca}^{2+} = 1:372$  (e) in Tris buffer containing 0.15 M NaCl.

two peaks at  $m/u = 502.4$  and  $541.7$  are observed. The peak at  $m/u = 502.4$  corresponds to a 1:1 complex of the form  $[\text{TC}^{2-} + \text{Ca}^{2+} + \text{H}_2\text{O} + \text{H}^+]^+$ , while the peak-group centered at  $541.7$  could correspond to a 1:2 ligand:metal complex.

### 3.5. Anhydrotetracycline Titration with $\text{Mg}^{2+}$ at pH 8.02.

In the absence of chelating metal ions, the CD spectrum of AHTC exhibits in the UV a weak negative band at about 230 nm and a broad positive band at about 270 nm (Figure 6a, solid line). The signal intensity of the negative peak in the visible ( $\sim 427$  nm) is weak (Figure 6b). Upon addition of  $\text{Mg}^{2+}$  up to a molar ratio of  $\text{AHTC}:\text{Mg}^{2+} = 1:372$ , a Cotton effect appears in the UV centered at about 260 nm, indicating that the broad band at about 268 nm is of a composite nature and that complexation with  $\text{Mg}^{2+}$  induces a conformational change of AHTC.

The UV-VIS absorption spectrum of AHTC shows relatively small spectral alterations upon addition of  $\text{Mg}^{2+}$  (Figure 6c). The absorption maximum at 430 nm shifts to 440 nm after addition of a 200-fold molar excess of  $\text{Mg}^{2+}$  ions (Figure 6d).

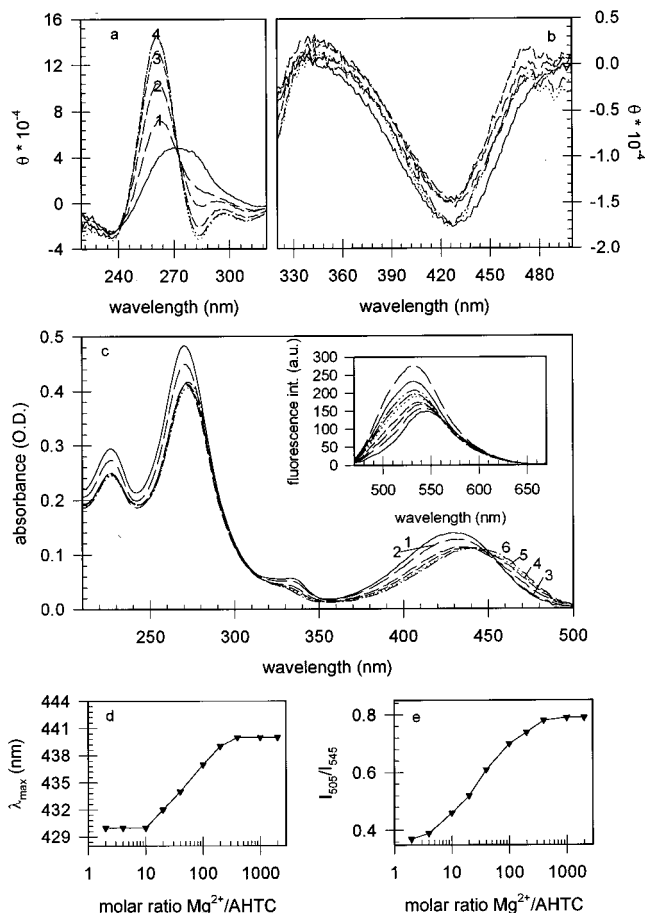


**Figure 6.** CD-spectra (a, b) of AHTC ( $2.1 \times 10^{-5}$  M) in the absence (solid line) and in the presence of increasing  $\text{Mg}^{2+}$  concentrations. The molar ratios of  $\text{TC}:\text{Mg}^{2+}$  are: (1) 1:5, (2) 1:10, (3) 1:30, and (4) 1:372. (c) Absorption spectra of  $\text{TC}:\text{Mg}^{2+}$  solutions exhibiting molar ratios of (1) 1:0, (2) 1:10, (3) 1:40, (4) 1:100, (5) 1:200, and (6) 1:1000. Inset: Fluorescence emission spectra ( $\lambda_{\text{exc}} = 450$  nm) of  $\text{AHTC}:\text{Mg}^{2+}$  solutions exhibiting molar ratios of (1) 1:0, (2) 1:10, (3) 1:20, (4) 1:40, (5) 1:100, (6) 1:200, (7) 1:400, (8) 1:1000, and (9) 1:2000 (from the bottom to the top). (d) Peak position of the long wavelength absorption band of  $\text{AHTC}:\text{Mg}^{2+}$  solutions as a function of the molar ratio  $\text{Mg}^{2+}/\text{TC}$ . (e) Fluorescence intensity ratio ( $I_{505}/I_{545}$ ) of  $\text{AHTC}:\text{Mg}^{2+}$  solutions ( $\lambda_{\text{exc}} = 346$  nm) as a function of the molar ratio  $\text{Mg}^{2+}/\text{TC}$ .

This shift is accompanied by a decrease in the absorbance. In addition, the absorption band at about 335 nm weakens, and there is a general decrease in the absorbance in the 200–300 nm wavelength region.

The fluorescence intensity increases upon chelation by a factor of 2 and the emission maximum is blue shifted from 544 to 531 nm (inset of Figure 6c). In addition, a shoulder forms on the short wavelength side of the band at about 505 nm. The dependence of the fluorescence intensity ratio ( $I_{505}/I_{545}$ ) on the  $\text{Mg}^{2+}$  concentration shows sigmoidal behavior with an inflection point at a molar ratio of approximately 1:60 (Figure 6e).

### 3.6. Anhydrotetracycline Titration with $\text{Ca}^{2+}$ at pH 8.02.

Chelation with  $\text{Ca}^{2+}$  leads only to small alterations of the CD (Figure 7 a,b), absorption (Figure 7c), and emission (inset of Figure 7c) spectra. The broad positive CD band in the UV at about 268 nm narrows upon addition of  $\text{Ca}^{2+}$ , and the formation of a slight shoulder is detected at molar ratios  $\text{AHTC}:\text{Ca}^{2+} \geq 1:400$  (Figure 7a). These alterations support the assumption that the broad CD band in the UV is of a composite nature.

The long wavelength absorption band shifts from 430 to 436 nm, while the position of the absorption bands in the region between 200 and 350 nm remain unchanged (Figure 7c). In

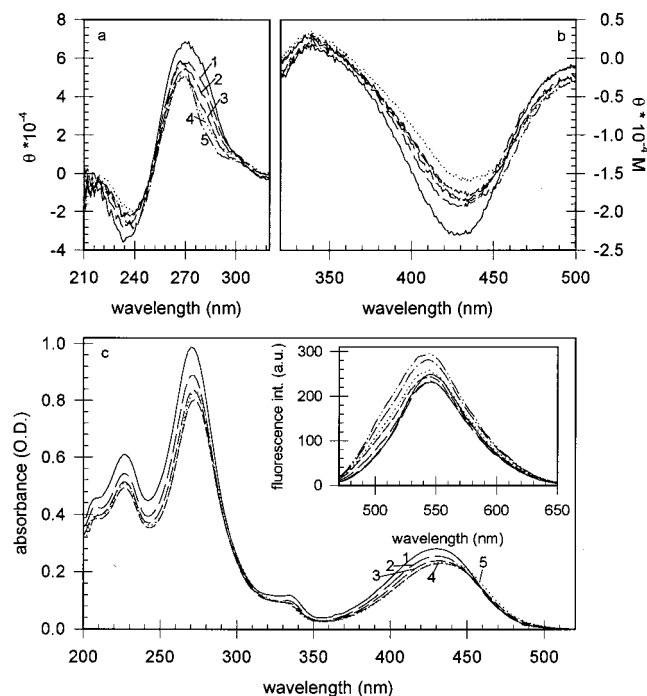


**Figure 7.** CD-spectra (a, b) of AHTC ( $2.1 \times 10^{-5}$  M) in the absence (solid line) and in the presence of increasing  $\text{Ca}^{2+}$  concentrations. The molar ratios of TC: $\text{Ca}^{2+}$  are (1) 1:10, (2) 1:40, (3) 1:100, (4) 1:400, and (5) 1:1000. (c) Absorption spectra of TC: $\text{Ca}^{2+}$  solutions exhibiting molar ratios of (1) 1:0, (2) 1:10, (3) 1:40, (4) 1:100, and (5) 1:400. Inset: Fluorescence emission spectra ( $\lambda_{\text{exc}} = 450$  nm) of AHTC: $\text{Ca}^{2+}$  solutions exhibiting molar ratios of (1) 1:0, (2) 1:10, (3) 1:40, (4) 1:200, (5) 1:400, (6) 1:1000, and (9) 1:2000.

addition, the peak position of the fluorescence emission band remains constant upon addition of  $\text{Ca}^{2+}$  (inset of Figure 7c). The fluorescence intensity increases by approximately 20–30%, and the formation of a shoulder at the short wavelength side is observed.

**3.7. TOF–SIMS Measurements of AHTC in the Presence of  $\text{Mg}^{2+}$ .** The results of the TOF–SIMS measurements are shown in Figure 8. In a NaCl-free TRIS buffer (pH 8.02) a pronounced signal appears in the positive TOF–SIMS at  $m/u = 427$  (Figure 8a), which corresponds to the protonated form of AHTC ( $\text{AHTCH}^+$ ). In the presence of excess  $\text{Na}^+$  the peak appears at  $m/u = 449$  (Figure 8b). As with TC, this signal can be attributed to a complex between AHTC and  $\text{Na}^+$ ,  $[\text{AHTC} + \text{Na}]^+$ . Upon addition of a 372 molar excess of  $\text{Mg}^{2+}$  in addition to the peak corresponding to  $\text{AHTCH}^+$  a second peak at  $m/u = 897.6$  (Figure 8c) appears. This peak could correspond to a 2:2 complex of the form  $[2(\text{AHTC}^{2-}) + 2\text{Mg}^{2+} + \text{H}]^+$ .

#### 4. Discussion

**4.1. Binding of TC with  $\text{Ca}^{2+}$ .** TC consists of two chromophoric systems which are separated from each other by the C12a–C4a bond. The absorption spectrum of TC (Figure 1c) exhibits three maxima (pH 8: 219, 274, and 368 nm). According to McCormik et al., the  $\pi$ – $\pi^*$  transitions of the BCD ring system contribute to all three absorption maxima of TC, whereas the  $\pi$ – $\pi^*$  transition of the  $\beta$ -tricarboxyl system of ring A contributes only to the absorption band at 274 nm.<sup>35</sup> It has been established that the two chromophoric systems have different orientations relative to each other depending on the state of protonation and/or complexation.<sup>11,14,19,25</sup> The three macroscopic  $pK$  values of TC in aqueous solution are  $pK_1 \sim 3.3$ ,  $pK_2 \sim 7.6$ , and  $pK_3 \sim 9.2$ ; these have been assigned to

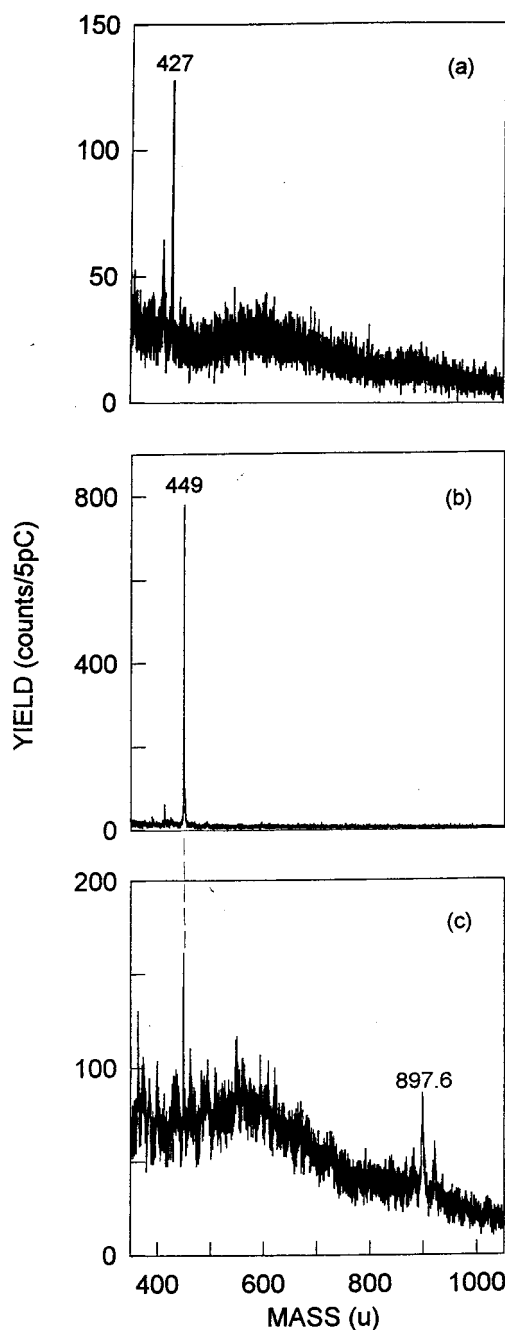


**Figure 8.** Positive TOF–SIMS spectra of AHTC ( $2.1 \times 10^{-5}$  M) (a), AHTC: $\text{Mg}^{2+} = 1:372$  (b), and AHTC: $\text{Ca}^{2+} = 1:372$  (c) in Tris buffer containing 0.15 M NaCl.

OH3, OH12, and the protonated nitrogen of the dimethylamino group, respectively.<sup>36</sup> Thus it can be assumed that at pH 8.02, O3 is fully deprotonated and that O12 is also predominantly deprotonated (roughly 70% in metal-free solution). Since N4 is to a large extent (about 90%) protonated at pH 8.02 and the negative charge from deprotonation of O3 is delocalized over the conjugated  $\pi$ -system of the A-ring chromophore, the majority of the TC molecules adopt a twisted conformation (B) (Scheme 2) to relieve steric crowding between OH12a and the protonated dimethylamino group.<sup>9,14,15,25,37</sup> In this conformation the CD spectrum exhibits one negative band in the UV which peaks at 263 nm (Figure 1a).

Upon addition of  $\text{Ca}^{2+}$  an additional Cotton effect develops in the UV (Figure 1a). CD spectroscopic studies performed in aqueous solution as a function of pH and in nonaqueous solution confirm that the formation of a new Cotton effect in the UV is

indicative for a conformational change of TC.<sup>12,15</sup> Hence, the formation of this additional Cotton effect indicates that complexation with  $\text{Ca}^{2+}$  induces conformation A of TC (Scheme 2). TC adopts this lower energy conformation also at high pH values and in organic solvents, where deprotonation of the dimethylamino nitrogen allows for hydrogen bonding between OH12a and N4,<sup>25</sup> which is most likely essential for the stabilization of conformation A. The second Cotton effect in the visible occurs concomitantly with the spectral alterations in the UV (Figure 2a). The appearance of this Cotton effect has been observed already by others<sup>9,11,15,38</sup> and is according to Newman and Frank indicative for a chelation involving both, the BCD- and the A-ring system.<sup>12</sup>

As noted above (section 3.1), two distinct types of  $\text{Ca}^{2+}$ -dependent absorption changes having different isosbestic points exist for molar ratios below and above  $\text{TC}:\text{Ca}^{2+} = 1:15.8$ . This indicates that binding of  $\text{Ca}^{2+}$  gives rise to two different equilibria. The  $\text{Ca}^{2+}$  dependence of the absorption spectra further suggests that a 1:2 ligand:metal complex is formed at high  $\text{TC}:\text{Ca}^{2+}$  ratios (Figure 2b). The  $\text{Ca}^{2+}$  dependence of the integrated fluorescence intensity ( $I_{\text{INT}}$ ), however, shows only one inflection point, which is probably due to the fact that the uncomplexed TC is essentially nonfluorescent, and both complexed forms exhibit similar fluorescence properties.

With respect to the fact that the structure of the absorption spectrum in the UV region remains unchanged upon addition of  $\text{Ca}^{2+}$  for  $\text{TC}:\text{Ca}^{2+} \leq 1:15.8$ , the bathochromic shift of the long wavelength absorption band for  $\text{TC}:\text{Ca}^{2+} \leq 1:15.8$  (Figure 1c) indicates that  $\text{Ca}^{2+}$  binds first to the BCD ring system. The BCD ring system has been widely suggested as the first chelation site, although the exact position is disputed.<sup>11,12,16,29,39</sup> Since O12 is to a large extent deprotonated at pH 8, it is likely to be involved in the chelation.<sup>36</sup>

Based on the CD spectra (Figure 1a) the second chelation site involves both the A- and BCD-ring systems (vide supra). According to Bhatt and Jee, who studied the micro-deprotonation scheme of TC via fluorescence emission measurements in water, the pK values for deprotonation of the dimethylamino nitrogen (pK 7.96) and OH12 (pK 7.82) are both close together and below 8.<sup>36</sup> The acidities of these sites effectively increase in the presence of divalent cations, which compete with the protons for binding (vide supra),<sup>37,38</sup> because the pK value of any particular site depends on the degree of protonation of the others.<sup>39,40</sup> This interdependence of pK values is largest between the sites on rings A and C.<sup>40</sup> Thus, we suggest that under the chosen experimental conditions, the quaternary amino group deprotonates in the presence of divalent cations and hence allows TC to adopt conformation A. In this conformation O12 and O1 are in the same plane and are, therefore, available as a coordination site for the second  $\text{Ca}^{2+}$  ion which leads to the formation of the Cotton effect in the visible. Consequently, in the 1:2 ligand:metal complex, the other  $\text{Ca}^{2+}$  ion most likely chelates through O10–O11 as a result of tautomerization.<sup>2,38,40,41</sup> These proposed binding sites agree with those suggested by Newman and Frank<sup>12</sup> as well as Jogun and Stezowski.<sup>37</sup> The results obtained from the TOF–SIMS measurements (section 3.4) support the assumption that under the chosen experimental conditions in the presence of a high molar excess of  $\text{Ca}^{2+}$  two  $\text{Ca}^{2+}$  ions chelate with TC (Figure 5c).

According to Lambs et al.,  $\text{Ca}^{2+}$  binds to TC in aqueous solution only at pH values  $\text{pH} \geq 9$ , when the nitrogen of the dimethylamino group is not protonated.<sup>15</sup> They suggest that the chelation of the two  $\text{Ca}^{2+}$  ions occurs through the N4–OH12a and O12–O1 sites and that chelation of  $\text{Ca}^{2+}$  to N4–

OH12a is responsible for the induction of conformation A.<sup>15</sup> Binding of  $\text{Ca}^{2+}$  through N4–OH12a has also been discussed by Mitscher et al.<sup>7,11</sup> If, however, TC adopts a twisted conformation (B) in order to relieve steric crowding between the protonated N4 and OH12a groups, exchange of a proton by  $\text{Ca}^{2+}$  at N4 should only increase the steric crowding and hence lead to a stabilization of that conformation rather than to the induction of conformation A. Moreover, the  $\text{CH}_3$  groups on N4 are rather bulky, and hence it is questionable whether  $\text{Ca}^{2+}$  is small enough to access the N4 on the dimethylamino group.

The CD spectra of  $\text{TC}:\text{Ca}^{2+} = 1:164$  at pH values ranging from  $7.0 < \text{pH} \leq 8.02$  indicate that the equilibrium of the complexed TC shifts from conformation A back to conformation B if the pH decreases to values  $\text{pH} < 7.7$  (Figure 3a,b). In other words, if N4 is protonated due to the high proton concentration in solution, the steric interaction between the protonated dimethylamino nitrogen and OH12a is large enough to induce the conformational change. Again, two sets of absorption spectra are observed for pH values below and above pH 7.7 (vide supra). In addition the  $\text{Ca}^{2+}$ -induced formation of conformation A is apparent in the splitting of the absorption band at 274 nm which also starts to become evident only at  $\text{pH} > 7.7$ . Splitting of this band appears to be indicative for a complexation involving both chromophoric systems. Furthermore, the integrated fluorescence intensity ( $I_{\text{INT}}$ ) is saturated at  $\text{pH} > 7.7$ , indicating that under the chosen conditions two  $\text{Ca}^{2+}$  ions can chelate to TC above pH 7.7 (Figure 3e). This is evidence that in aqueous solution at a molar ratio of  $\text{TC}:\text{Ca}^{2+} = 1:164$ , the nitrogen on the dimethylamino group is to a significant extent deprotonated at  $\text{pH} > 7.7$ .

It is pertinent to note that the ratios of the fluorescence intensities at 532 and 502 nm (excited at 305 nm) exhibit an inflection point at pH 7.7 (Figure 3f), indicating that these peaks could result from the different TC conformations exhibiting different extinction coefficients at the excitation wavelength.

**4.1. Binding of TC with  $\text{Mg}^{2+}$ .** In contrast to  $\text{Ca}^{2+}$ , binding of  $\text{Mg}^{2+}$  stabilizes the zwitterionic conformation B (Scheme 2), since the negative CD band at about 272 nm becomes more negative upon binding of  $\text{Mg}^{2+}$  (Figure 4a). Based on the assumption that a stabilization of the twisted conformation is caused by an increase in the steric crowding between positively charged binding partners of N4 and OH12a (vide supra), the observed stabilization of conformation B indicates that one  $\text{Mg}^{2+}$  ion binds through N4 and O3 and thereby prevents TC from adopting conformation A. As in the case of  $\text{Ca}^{2+}$ ,  $\text{Mg}^{2+}$  induces a small bathochromic shift of the long wavelength absorption band and the appearance of a shoulder at high  $\text{Mg}^{2+}$  concentrations. These spectral changes could indicate that  $\text{Mg}^{2+}$  binds to the BCD ring system. However, binding to the A ring could also lead to such a shift as the result of an increase in the acidity of the O10–O11–O12 moieties as suggested by Riegler et al.<sup>40</sup>

N4–O3 and O11–O12 have both been discussed in the literature as possible binding sites for  $\text{Mg}^{2+}$ . Newman and Frank suggested that only one  $\text{Mg}^{2+}$  binds to TC through O11–O12 and that the A ring is not involved in chelation.<sup>12</sup> This conclusion was obtained via a comparison of the CD spectra from dedimethylamino TC in (1:1 MeOH/ $\text{H}_2\text{O}$ ) without  $\text{Mg}^{2+}$  and in (90/10 MeOH/ $\text{H}_2\text{O}$ ) in the presence of  $\text{Mg}^{2+}$ . Because of the change in solvent, a direct comparison of the signal intensities, however, is questionable in our opinion. According to Lambs et al., a 1:1  $\text{TC}:\text{Mg}^{2+}$  complex is predominant at pH 8, while at higher pH values a 1:2 complex is formed in which  $\text{Mg}^{2+}$  binds through O10–O12 and N4–O3.<sup>15</sup>

TOF–SIMS measurements (section 3.4), however, indicate that in the presence of a 372-fold molar excess of  $\text{Mg}^{2+}$  at pH



8.02, both, a 1:1 and a 1:2 metal:ligand complex is formed (Figure 5c) under the chosen experimental conditions. Thus we suggest that in the 1:1 complex  $\text{Mg}^{2+}$  binds to N4–O3 and that the observed shift of the long wavelength band can be attributed to binding of  $\text{Mg}^{2+}$  to the A-ring site. At high molar excess of  $\text{Mg}^{2+}$  a 1:2 ligand:metal complex is formed. The observed shoulder on the long wavelength absorption band (Figure 4c) and the observed pronounced increase in the integrated fluorescence intensity (Figure 4e) suggest that the other  $\text{Mg}^{2+}$  chelates to O12–O11.

**4.2. Binding of AHTC with  $\text{Ca}^{2+}$  and  $\text{Mg}^{2+}$ .** The absorption spectrum of AHTC in aqueous solution (pH 8.02) exhibits four peaks at about 228, 270, 335, and 430 nm (Figure 6b). As in the case of TC they are assigned to  $\pi$ – $\pi^*$  transitions of the aromatic BCD ring system. The A-ring chromophore contributes only to the absorption band at 270 nm.<sup>42,45</sup> The two chromophoric systems are also oriented differently relative to each other, but the C and D rings are more planar than in TC, leading to a less intense CD signal in the visible (Figure 6b).<sup>43</sup> In addition, differences in the A-ring conformations of AHTC and TC have been reported.<sup>44</sup> The three macroscopic  $\text{pK}$  values of AHTC in aqueous solution are at  $\text{pK}_1 = 3.2$ ,  $\text{pK}_2 = 5.9$ , and  $\text{pK}_3 = 8.5$  and have been assigned to OH3, OH10, and NH4, respectively.<sup>17</sup> Thus it can be assumed that O3 and O10 are fully deprotonated at pH 8.02.

According to the CD-spectroscopic studies of Machado et al. AHTC also adopts a twisted conformation (B) in its zwitterionic form in order to relieve the steric crowding between the protonated nitrogen on the dimethylamino group and OH12a. In this conformation the CD spectrum exhibits a negative peak at about 288 nm.<sup>17</sup> Under the chosen experimental conditions (pH 8.02), however, AHTC shows only one broad positive CD band at about 269 nm (Figure 6a), indicating that the equilibrium between the zwitterionic and extended conformations is shifted to the latter (conformation A), where N4 is deprotonated and hydrogen bonded to OH12a.

Upon addition of  $\text{Mg}^{2+}$  the broad positive band at 269 nm narrows and a negative band at 282 nm is formed, the intensity of which is saturated at a molar ratio of AHTC: $\text{Mg}^{2+} = 1:372$  (Figure 6a). This indicates that  $\text{Mg}^{2+}$  competes effectively with the hydrogen bonding between N4 and OH12a; binding at N4–O3 increases the steric crowding with OH12a and hence forces the A ring of AHTC into the twisted conformation B. Coordination with  $\text{Mg}^{2+}$  leads also to the formation of a shoulder at about 505 nm in the fluorescence emission spectra (inset Figure 6c). The ratio of the fluorescence intensity at 505 nm and at 545 nm (maximum of the uncomplexed AHTC) shows a similar dependence on the  $\text{Mg}^{2+}$  concentration as the peak position of the absorption maximum (430 nm) (Figure 6d,e) and increases in the same molar ratio range where the negative band in the CD spectrum develops (Figure 6a). This indicates that the change in the shape of the emission spectrum is due to the induction of a new AHTC conformation (Figure 6b).

In the same molar ratio region a bathochromic shift (430 nm  $\rightarrow$  441 nm) of the visible absorption maximum is observed (Figure 6c,d). As in the case of TC, this shift can either be due to chelation of another  $\text{Mg}^{2+}$  ion to the BCD ring system, i.e., when a ligand:metal = 1:2 complex is formed, or result from the enhanced acidity of the BCD moiety due to binding on the A-ring site in a ligand:metal = 1:1 complex (vide supra). According to the theoretical investigations of DeAlmedia et al., the weak absorption band at 335 nm is present only when O10 is deprotonated.<sup>45</sup> Therefore the  $\text{Mg}^{2+}$  induced disappearance

of the shoulder at 335 nm (Figure 6b) could indicate that the deprotonated O10 is also involved in complexation.

Machado et al. observed the formation of 1:1 and 1:2 ligand:metal complexes and suggested O11 as the primary binding site and N4–O3 as the secondary one.<sup>17</sup> According to Stoel et al., however, metal ions chelate through O11, while A-ring chelation occurred only when the primary binding site (O11) was blocked.<sup>30</sup> This binding site, however, does not account for the observed conformational alterations.

TOF–SIMS measurements indicate that a 1:1 and a 2:2 ligand:metal complex is formed under the chosen experimental conditions (Figure 8c). The dimer can be visualized as a complex which is formed through chelation at N4–O3 on AHTC(I) and O10–O11 on AHTC(II) and vice versa. This kind of dimer can thus account for the above-described alterations in the absorption spectrum at 335 nm. The formation of octahedral complexes involving one metal ion and two tetracyclines has been suggested by Mitscher et al.<sup>10</sup>

In contrast to  $\text{Mg}^{2+}$ , addition of  $\text{Ca}^{2+}$  causes only a slight narrowing of the positive band at 269 nm (Figure 7a). The small bathochromic shift (430 nm  $\rightarrow$  436 nm) of the long wavelength absorption band is less pronounced (Figure 7b) and the shape of the fluorescence emission spectrum does not change upon addition of  $\text{Ca}^{2+}$  (inset of Figure 7b). The CD-spectra do not provide evidence for pronounced conformational changes and hence it can be assumed that the N4 is not involved in the chelation of  $\text{Ca}^{2+}$ . Since chelation has little effect on the absorption in the region of the shoulder at 335 nm, O10 is most likely not involved in binding.<sup>45</sup> Although the observed bathochromic shift of the long wavelength absorption band is small and the increase in the fluorescence intensity is only marginal, it is likely that O11 is involved in chelation, which is in agreement with the observations of Stoel et al.<sup>30</sup>

## Summary and Conclusion

The spectroscopic results presented in this contribution provide evidence that in aqueous buffer at pH 8.02 TC and AHTC differ in the state of protonation at N4. In TC, where the nitrogen on the dimethylamino group is protonated, the steric interaction with OH12a is large enough to induce the twisted conformation, whereas AHTC exists in the basic form and adopts the extended conformation (A). Due to this difference in conformation, the effect of interaction with divalent ions is also different for both compounds. In addition the chelation behaviors of TC and AHTC depend on the size of the ions. Because  $\text{Mg}^{2+}$  is small enough, it can chelate with N4–O3 and stabilize (in the case of TC) or induce (in the case of AHTC) the twisted conformation B. In case of TC it is postulated that chelation of  $\text{Ca}^{2+}$  at O11–O12 leads to a deprotonation of the nitrogen on the dimethylamino group and hence to the induction of conformation A which is stabilized via hydrogen bonding between N4 and OH12a. pH titrations provide evidence that deprotonation of the dimethylamino nitrogen occurs at pH > 7.7. In the case of AHTC, chelation with  $\text{Ca}^{2+}$  leads to a stabilization of conformation A. At higher metal ion concentrations the formation of 2:1 metal:TC complexes are postulated, the complexation sites being dependent on the size of the ions. In the case of AHTC, no strong evidence was found for this type of larger complexes. TOF–SIMS suggests the existence of  $(\text{AHTC}/\text{Mg}^{2+})_2$  dimers, in which O10 is involved in the binding. The reported findings seem to bear importance for binding studies of TC to proteins such as the Tet Repressor protein Tet R. In these studies it is usual to work with high excess of divalent ions, and to assume the existence of 1:1 complexes only.

**Acknowledgment.** The authors thank Prof. H. Scheer (LMU, München) for providing access to his CD spectrometer. Financial support by the Deutsche Forschungsgemeinschaft and Fonds der Chemischen Industrie is also gratefully acknowledged.

## References and Notes

- (1) Mitscher, L. A. *The Chemistry of Antibiotics*; Marcel Dekker: New York, 1978; p 91.
- (2) Kohn, K. W. *Nature* **1961**, *191*, 1156.
- (3) Dürckheimer, W. *Angew. Chem.* **1975**, *21*, 751.
- (4) Williamson, D. E.; Everett, G. W., Jr. *J. Am. Chem. Soc.* **1975**, *97*, 2397.
- (5) Everett, G. W., Jr.; Gulbis, J.; Shaw, J. J. *Am. Chem. Soc.* **1982**, *104*, 445.
- (6) Gulbis, J.; Everett, G. W., Jr. *Tetrahedron* **1976**, *32*, 913.
- (7) Mitscher, L. A.; Bonacci, A. C.; Sokoloski, T. D. *Tetrahedron Lett.* **1968**, *51*, 5361.
- (8) Celotti, M.; Fazakerley, G. V. *J. Chem. Soc., Perkin Trans. 2* **1977**, 1319.
- (9) Mitscher, L. A.; Bonacci, A. C.; Sokoloski, T. D. *Antimicrob. Agents Chemother.* **1968**, 78.
- (10) Mitscher, L. A.; Bonacci, A. C.; Slater-Eng, B.; Hacker, A. K.; Sokoloski, T. D. *Antimicrob. Agents Chemother.* **1969**, 111.
- (11) Mitscher, L. A.; Slater-Eng, B.; Sokoloski, T. D. *Antimicrob. Agents Chemother.* **1972**, *2*, 66.
- (12) Newman, E. C.; Frank, C. W. *J. Pharm. Sci.* **1976**, 1728.
- (13) Prewo, R.; Stezowski, J. J. *J. Am. Chem. Soc.* **1980**, *102*, 7015.
- (14) Hughes, L. J.; Stezowski, J. J.; Hughes, R. E. *J. Am. Chem. Soc.* **1979**, *101*, 7655.
- (15) Lambs, L.; Decock-Le Révérend, B.; Kozłowski, H.; Berthon, G. *Inorg. Chem.* **1988**, *27*, 3001.
- (16) Jezowska-Bojczuk, M.; Lambs, L.; Kozłowski, H.; Berthon, G. *Inorg. Chem.* **1993**, *32*, 428.
- (17) Machado, F. C.; Demicheli, C.; Garnier-Suillerot, A.; Beraldo, H. *J. Inorg. Biochem.* **1995**, *60*, 163.
- (18) Baker, W. A., Jr.; Brown, P. M. *J. Am. Chem. Soc.* **1966**, *88*, 1314.
- (19) Caswell, A. H.; Hutchison, J. D. *Biochem. Biophys. Res. Commun.* **1971**, *43*, 625.
- (20) Sachan, N. P.; Gupta, C. M. *Talanta* **1980**, *27*, 457.
- (21) Brion, M.; Berthon, G.; Fourtillan, J.-B. *Inorg. Chim. Acta* **1981**, *55*, 47.
- (22) Sharma, R. K.; Joseph, S. *Indian J. Chem.* **1996**, *35A*, 639.
- (23) Terada, H.; Inagi, T. *Chem. Pharm. Bull.* **1975**, *23*, 1960.
- (24) Prewo, R.; Stezowski, J. J. *J. Am. Chem. Soc.* **1976**, *98*, 1117.
- (25) Martin, R. B. In *Metal Ions in Biological Systems*; Siegel, H., Ed.; Marcel Dekker: New York, 1985; Vol. 19, pp 20–52.
- (26) Stezowski, J. J. *J. Am. Chem. Soc.* **1977**, *99*, 1122.
- (27) Robinson, R. A.; Stokes, R. H. In *Electrolyte Solutions*; 2nd ed. Butterworth: London, 1959; p 517.
- (28) Leeson, L. J.; Krueger, J. E.; Nash, R. A. *Tetrahedron Lett.* **1963**, *18*, 1155.
- (29) Helena Mendça Dias, M.; Fraústo da Silva, J. J. R.; Xavier, A. V. *Rev. Port. Quím.* **1979**, *21*, 5.
- (30) Stoel, L. J.; Newman, E. C.; Asleson, G. L.; Frank, C. W. *J. Pharm. Sci.* **1976**, *65*, 1794.
- (31) De Siqueira, J. M.; Carvalho, S.; Paniago, E. B.; Tosi, L.; Beraldo, H. *J. Pharm. Sci.* **1993**, *83*, 291.
- (32) Degenkolb, J.; Takahashi, M.; Ellestad, G. A.; Hillen, W. *Antimicrob. Agents Chemother.* **1991**, *35*, 1591.
- (33) Szymczak, W.; Wittmaack, K. *Phys. Res. B* **1994**, *88*, 149.
- (34) Gulbis, J.; Everett, G. W.; Frank, C. W. *J. Am. Chem. Soc.* **1976**, *98*, 1280.
- (35) McCormick, J. R. D.; Fox, S. M.; Smith, L. L.; Bitler, B. A.; Reichenthal, J.; Origoni, V. E.; Muller, W. H.; Winterbottom, R.; Doerschuk, A. P. *J. Am. Chem. Soc.* **1957**, *79*, 2849.
- (36) Bhatt, V. K.; Jee, R. D. *Anal. Chim. Acta* **1985**, *167*, 233.
- (37) Jogun, K. H.; Stezowski, J. J. *J. Am. Chem. Soc.* **1976**, *98*, 6018.
- (38) Day, S. T.; Crouthamel, W. G.; Martinelli, L. C.; Ma, J. K. H. *J. Pharm. Sci.* **1978**, *67*, 1518.
- (39) Martin, S. R. *Biophys. Chem.* **1979**, *10*, 319.
- (40) Rigler, N. E.; Bag, S. P.; Leyden, D. E.; Sudmeier, J. L.; Reilley, C. N. *Anal. Chem.* **1965**, *37*, 872.
- (41) Morrison, H.; Olack, G.; Xiao, C. *J. Am. Chem. Soc.* **1991**, *113*, 8110.
- (42) Harrada, N.; Nakanishi, K.; Tatsuoka, S. *J. Am. Chem. Soc.* **1969**, *91*, 5896.
- (43) Palenik, G. J.; Mathews, M.; Restivo, R. *J. Am. Chem. Soc.* **1978**, *100*, 4458.
- (44) Restivo, R.; Palenik, G. J. *Biochem. Biophys. Res. Commun.* **1969**, *36*, 621.
- (45) De Almedia, W. B.; Costa, L. R. A.; Dos Santos, H. F.; Zerner, M. C. *J. Chem. Soc., Perkin Trans. 2* **1997**, 1335.